

## Axial Chiral Bisbenzophenazines: Solid-State Self-Assembly via Halide Hydrogen Bonds Triggered by Linear Alkanes

Alison E. Metz,<sup>§</sup> Erin E. Podlesny,<sup>§</sup> Patrick J. Carroll, Ariel N. Klinghoffer, and Marisa C. Kozlowski\*

Department of Chemistry, University of Pennsylvania, Philadelphia, Pennsylvania 19104, United States

## Supporting Information

**ABSTRACT:** An axial chiral tetrachlorinated bisbenzo[*a*]phenazine has been discovered that undergoes an alkane-induced shift in the solid state from a disordered amorphous form to an ordered polycrystalline form. This phase transition is caused by the formation of pores that accommodate linear alkanes of varying lengths with a very strong affinity as judged by differential scanning calorimetry. Single crystal X-ray structure analysis revealed that a series of weak phenolic OH...Cl hydrogen bonds dictates the pore structure. These weak interactions can be disrupted mechanically, causing the material to revert to the amorphous form. Notably, the interchange between the amorphous and crystalline forms is readily reversible and is easily observed by characteristic colorimetric changes. Measurements via photoimage processing reveal that the degree of color change is dictated by the type of alkane employed.

Phenazines are redox-active compounds containing an anthracenyl ring system with a pyrazine core. Phenazines<sup>1–3</sup> and the related pyrazine heterocycles have been developed as dyes,<sup>4</sup> heavy metal detectors,<sup>5</sup> semiconductors,<sup>6</sup> fluorescent probes, organic-light emitting diodes (OLEDs),<sup>7,8</sup> and sensors.<sup>9–11</sup> In addition, the acidochromism and photophysical properties have been reported recently for a number of benzo[*a*]phenazines.<sup>12,13</sup> The condensation reaction between a phenylenediamine and a quinone provides ready access to phenazines. Through this synthetic strategy, we envisioned formation of several axial chiral BINOL-based phenazine derivatives from the corresponding binaphtho-*o*-quinone.<sup>14</sup> One of the bisbenzo[*a*]phenazines synthesized during this effort exhibited mechanochromic<sup>15</sup> behavior, which was reversible upon exposure to solvent or solvent vapors. The mechanochromism and color changes triggered by small organic molecules could be utilized in the areas of materials chemistry and sensor development. Herein, we overview several phenazines and describe the unique properties and solid-state structure of an axial chiral tetrachlorinated derivative.

Several axial chiral bisbenzo[*a*]phenazines were generated in 7 steps and 13–19% overall yield<sup>16</sup> (Figure 1). The syntheses commence with an enantioselective vanadium-catalyzed naphthol coupling reaction.<sup>17–21</sup> Trituration of the resultant binaphthol provided 99% ee material. Selective oxidation afforded the binaphtho-*o*-quinones,<sup>14</sup> which were combined with phenylenediamines yielding **1a–f** and **3**. Similar axial chiral heterocyclic structures have not been reported, although

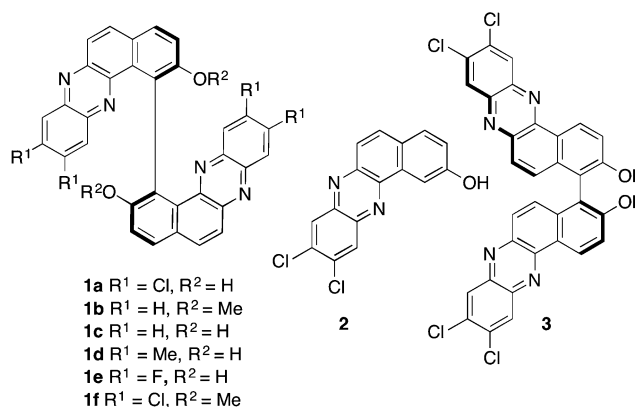
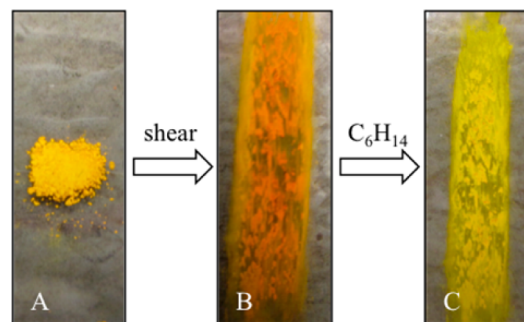


Figure 1. New benzophenazines.

a few carbon-based homologues have been studied.<sup>22–24</sup> Bisphenazine-based helicenes,<sup>25</sup> biaryl derivatives,<sup>26</sup> and an axially chiral bisacridine<sup>27</sup> are other relevant examples. The in-regiochemistry of **1b** was verified from the crystal structure of the racemate.<sup>16</sup>

Precipitation of tetrachlorinated **1a** from a solution in acetone with hexanes generated a yellow solid (Y-O, Figure 2A) that was found to be mechanochromic. Specifically, shearing the sample between glass slides led to a color change from yellow-orange to red-orange (R-O, Figure 2B). This characteristic was not seen with **1b–f**, **2**, or **3**, indicating that the chloro groups, phenol groups, dimeric assembly, and regiochemistry are all critical to this property. The <sup>1</sup>H NMR spectrum of Y-O



**Figure 2.** Mechanochromism of **1a**. (A) Solid before shearing (Y-O form). (B) Production of R-O form by shearing. (C) Reversal of R-O solid to the Y-O solid by suspension in *n*-hexane.


Received: June 18, 2014

Published: July 14, 2014

revealed a complex with hexane, and the spectrum of R-O confirmed that **1a** remains intact. In addition to production of R-O by mechanical stress, concentration of **1a** from a homogeneous solution in MeOH also produces R-O. Interestingly, the effect of the mechanical action could be reversed with solvent. Exposure of the sheared solid (or R-O obtained from MeOH) to alkane solvent or vapor reverts the sample to the Y-O form (Figure 2C).

Although not soluble in hydrophobic solvents, **1a** underwent characteristic color changes when exposed to such solvents (Table 1). Because these color changes occur in the solid phase,

**Table 1.** Colorimetric Response of R-O to Reagents

Entry	Reagent	Mean green light intensity <sup>a</sup>	Observed Color
1	perfluorohexane, R	41	
2	perfluorooctane	49	
3	cyclohexane	53	
4	methanol, R-O	77	
5	2-butyne	91	
6	2-methylpentane	105	
7	<i>cis</i> -2-hexene	107	
8	carbon disulfide	107	
9	<i>trans</i> -2-hexene	110	
10	deutero-octane	111	
11	1-hexene	118	
12	<i>n</i> -hexane, Y-O	118	
13	tridecane	118	
14	<i>n</i> -octane	120	

<sup>a</sup>Numbers are an average of two trials.

quantification was not possible via UV-vis spectroscopy. Diffuse-reflectance UV-vis spectroscopy was also not suitable; the mechanochromism precluded grinding the materials into powders needed for measurement. Instead, the color changes were quantified using photoimage processing (Table 1).<sup>28–30</sup> The mean green light intensity of the images was studied since red combined with green produces yellow. Samples with a stronger green light intensity in photos correspond to those with a more yellow appearance.

Commencing from the R-O form, color changes from red-orange to yellow were labeled a positive response, whereas changes to red were labeled a negative response (Figure 3). The color of the R-O material appears at a mean green light intensity of 77 (Table 1, entry 4). Fluorinated alkanes give a

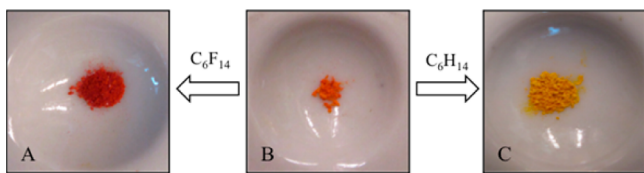


**Figure 3.** Solvatochromism of **1a**. (A) A negative response is obtained when R-O is exposed to perfluoroalkanes (solid becomes more red). (B) R-O produced by concentration of **1a** from MeOH. (C) A positive response occurs when R-O is exposed to linear alkanes (solid becomes more yellow).

negative response (entries 1 and 2; Figure 3A), while saturated linear alkanes produced a positive response (entries 12–14; Figure 3C). Interestingly, branched alkanes do not produce as strong a response as their linear isomers (entry 6 versus 12). Notably, tetracosane (C<sub>24</sub>H<sub>50</sub>) produces a positive response (not shown); however, this solid has to be first dissolved in cyclohexane. Gaseous molecules such as butane failed to cause any response. Overall, the strongest response arises from linear alkanes.

A similar color change upon exposure to solvent or solvent vapor has been reported for mechanochromic crystals of a benzo[*c*]thiophene derivative and was related to polymorphism.<sup>31</sup> On this basis, we hypothesized that the Y-O and R-O forms were due to color polymorphism, which may arise from structural variations in the solid state.<sup>32,33</sup> However, X-ray powder diffraction (XRPD)<sup>34</sup> of **1a** did not reveal two crystalline polymorphs. Rather, Y-O was found to be crystalline and R-O amorphous.<sup>16</sup> This result provides a qualitative explanation for the observed mechanochromism of **1a**: specifically, disruption of the crystal lattice during shearing creates an amorphous form, which is accompanied by a color change from yellow-orange to red-orange. The XRPD spectra revealed a similar crystalline polymorph for **1a** with all linear alkanes (see representative spectra in Figure 4).<sup>16</sup> Notably, the formation of a crystalline material is not observed by XRPD when **1a** is subjected to cyclohexane.

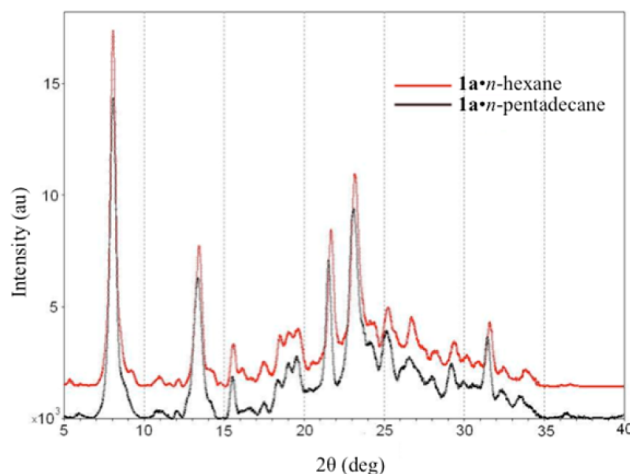


**Figure 4.** X-ray powder diffraction of the Y-O forms **1a**·*n*-hexane (red) and **1a**·*n*-pentadecane (black).

In order to understand the structural features giving rise to the observed mechanochromism and its reversibility, single crystal X-ray analysis was undertaken. The yellow-orange crystals of **1a**·*n*-hexane revealed a complex packing arrangement and network of intermolecular hydrogen bonds with a total of four symmetry-independent forms of bisphenazine **1a** (A, B, C, D) in the asymmetric unit. Notably, these molecules pair together (A and B or C and D), assembling around one molecule of hexane (Figure 5A), which explains the role of hexanes in initiating crystallization. Each of these dimeric assemblies, A/B and C/D, forms separate layers in the packing diagram (Figure 5B). A complex arrangement of intermolecular O–H···Cl and O–H···N hydrogen bonds stabilizes each layer (Figure 5C). The network of O–H···Cl bonds ( $d = 2.70–2.88$  Å;  $\theta = 130.5–140.0^\circ$ ) occurs between two symmetry-equivalent molecules, meaning A is hydrogen bonded only to

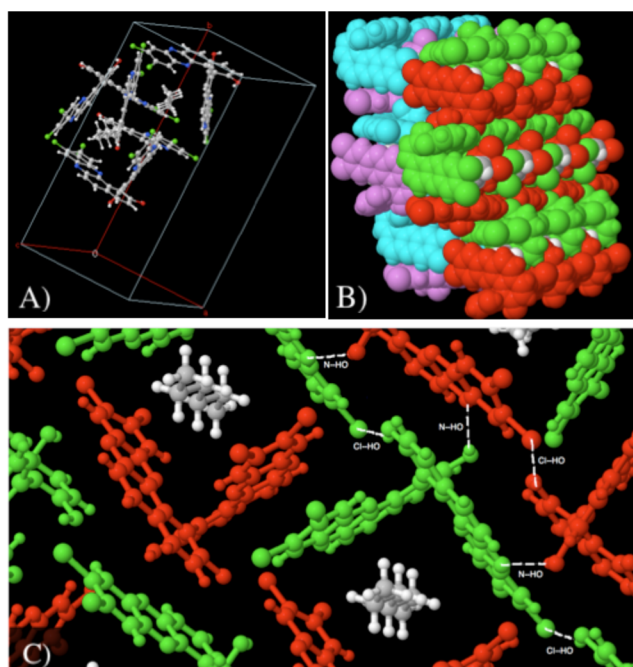


**Figure 5.** Crystal structure of **1a**-hexane. (A) Asymmetric unit of the crystal structure of **1a**. (B) A/B and C/D layers in the crystal structure of **1a**. (C) Network of intermolecular O–H...Cl and O–H...N hydrogen bonds for the A/B molecule layer.

other molecules of A, B to B, etc. However, the O–H...N hydrogen bonding ( $d = 2.03\text{--}2.37 \text{ \AA}$ ;  $\theta = 112.9\text{--}159.3^\circ$ ) occurs between two symmetrically different molecules within the same layer (A/B or C/D).

Notably, the packing diagram of **1a**-*n*-hexane shows that the pores are not aligned to allow a larger alkane to thread through two pores. To further understand how longer alkanes can cause similar XRPD and color changes, single crystal X-ray analysis was undertaken with a **1a**-*n*-tridecane crystal. This structure was found to differ from that of **1a**-*n*-hexane by the presence of only two symmetry-independent molecules (A and B) in the unit cell of the crystal, which again pair together (Figure 6A). Again, a network of intermolecular hydrogen bonds organizes the structure. The O–H...Cl interactions ( $d = 2.80\text{--}2.83 \text{ \AA}$ ;  $\theta = 145.2\text{--}151.2^\circ$ ) are similar, occurring between symmetry equivalent molecules. In contrast to the *n*-hexane adduct, O–H...O–H hydrogen bonds ( $d = 2.07\text{--}2.10 \text{ \AA}$ ;  $\theta = 167.2\text{--}168.6^\circ$ ) are seen between symmetrically different molecules in the same layer, such that A/B and A'/B' share O–H...O–H interactions. The O–H...O–H vs O–H...N hydrogen bonding network shifts the molecular pores into alignment to accommodate the longer alkane chain (Figure 6A and B), thereby creating a more symmetrical unit cell.

The weak intermolecular O–H...Cl–C interactions found in these structures are not common. A CSD (Cambridge Structural Database) study found only 5% of compounds containing both O–H and Cl–C groups have such intermolecular interactions.<sup>35</sup> Chlorines bound to carbon are less adequate acceptors than free chloride ions or those bound to metals.<sup>36</sup> Based on the long bond distances involved ( $>2.2 \text{ \AA}$ ), these hydrogen bonds are characterized as weak, but stabilizing (bond energies of 0.5–4 kcal/mol).<sup>35,37</sup>

A sample of **1a**-*n*-hexane placed under vacuum (5 Torr) overnight (15 h) does not change appearance and hexane is still observed by <sup>1</sup>H NMR, indicating a strong association between

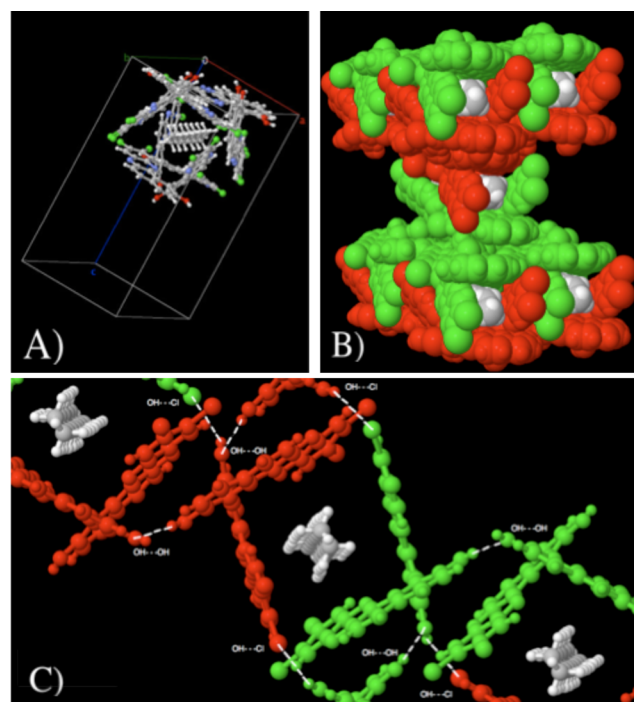


**Figure 6.** Crystal structure of **1a**-tridecane. (A) Phenazine molecules caging one tridecane. (B) Two A/B layers in the crystal structure. (C) Network of intermolecular O–H...Cl and O–H...O–H hydrogen bonding for the A/B molecular layer.

the alkane and the bisphenazine. Disassociation of hexane accompanied by a color change is only observed with heating. At temperatures above 200 °C, the sample gradually becomes the color of the R–O form and <sup>1</sup>H NMR reveals a loss of hexane. Remarkably, modulated differential scanning calorimetry of this nonreversible transition<sup>16</sup> revealed no transition until the onset of the primary transition at 190 °C.<sup>16</sup> Given the much lower boiling point of *n*-hexane (68 °C), the C–H... $\pi$  interactions between the arene faces of the pores of **1a** and *n*-alkanes appear highly stabilizing.

In summary, several axially chiral bisbenzo[*a*]phenazines have been synthesized, including two different regioisomers. The solvatochromism of a tetrachlorinated derivative in the solid phase was studied and quantified using photoimage processing. The mechanochromism of the compound was investigated and found to arise from the breakdown of the crystal lattice during the shearing process as judged by XRPD. X-ray crystallographic analysis reveals that the crystals are held together by weak O–H...Cl–C hydrogen bonds, forming a network of dimeric assemblies encapsulating alkane molecules. Additional properties of **1a** and the other phenazines, including fluorescence, acidochromism, and redox activity, have also been noted and further characterization is underway. The reversible mechanochromic properties of this compound could be valuable in the design of “smart” materials.<sup>38,39</sup> One example includes incorporating mechanochromic compounds into polymers providing an optical response to external stress, which would be useful in assessing the structural integrity of plastics. We are also investigating the use of this material in metal-free rewritable media.<sup>40–42</sup>

**■ ASSOCIATED CONTENT****■ Supporting Information**

Experimental procedures, characterization, NMR, X-ray powder diffraction, differential scanning calorimetry, photoimage processing, and single crystal X-ray data. This material is available free of charge via the Internet at <http://pubs.acs.org>.

**■ AUTHOR INFORMATION****Corresponding Author**

marisa@sas.upenn.edu

**Author Contributions**

<sup>§</sup>A.E.M. and E.E.P. contributed equally to this work.

**Notes**

The authors declare no competing financial interest.

**■ ACKNOWLEDGMENTS**

Financial support for this work was provided by the NSF (CHE1213230). E.E.P. gratefully acknowledges an NRSA predoctoral fellowship (F31-GM093515). Partial instrumentation support was provided by the NIH for MS (1S10RR023444) and NMR (1S10RR022442) and the NSF for X-ray (CHE 0840438). From UPenn, we thank Danielle Reifsnnyder, Taejong Paik, and Christopher Murray for XRPD training and Ethan Glor and Zahra Fakhraai for DSC assistance. From PennState, we thank Matthew Baker and Scott Phillips for discussions of photoimage processing. We also acknowledge David Chenoweth (UPenn) as well as Narayan Variankaval, Andrew Brunskill, and Chris Welch (Merck) for insightful discussions.

**■ REFERENCES**

- (1) Laursen, J. B.; Nielsen, J. *Chem. Rev.* **2004**, *104*, 1663.
- (2) Makgatho, M. E.; Anderson, R.; O'Sullivan, J. F.; Egan, T. J.; Freese, J. A.; Cornelius, N.; van Rensburg, C. E. J. *Drug Dev. Res.* **2000**, *50*, 195.
- (3) Dai, J.; Punchihewa, C.; Mistry, P.; Ooi, A. T.; Yang, D. *J. Biol. Chem.* **2004**, *279*, 46096.
- (4) Berneth, H. Azine Dyes. In *Ullmann's Encyclopedia of Industrial Chemistry*, Electronic Release; Wiley-VCH: Weinheim, 2000.
- (5) Wan, M.; Zou, Y.; Tan, S.; Li, Y. *Poly. Adv. Technol.* **2010**, *21*, 256.
- (6) Murphy, A. R.; Fréchet, J. M. J. *Chem. Rev.* **2007**, *107*, 1066.
- (7) Son, H.-O.; Han, W.-S.; Wee, K.-R.; Yoo, D.-H.; Lee, J.-H.; Kwon, S. N.; Ko, J.; Kang, S. O. *Org. Lett.* **2008**, *10*, 5401.
- (8) Son, H.-O.; Han, W.-S.; Yoo, D.-H.; Min, K.-T.; Kwon, S.-N.; Ko, J.; Kang, S. O. *J. Org. Chem.* **2009**, *74*, 3175.
- (9) Thomas, S. W., III; Joly, G. D.; Swager, T. M. *Chem. Rev.* **2007**, *107*, 1339.
- (10) Aldakov, D.; Palacios, M. A.; Anzenbacher, P., Jr. *Chem. Mater.* **2005**, *17*, 5238.
- (11) Pauliukaite, R.; Ghica, M. E.; Barsan, M. M.; Brett, C. M. A. *Anal. Lett.* **2010**, 1588.
- (12) Singh, P.; Baheti, A.; Thomas, K. R. J. *J. Org. Chem.* **2011**, *76*, 6134.
- (13) Khurana, J. M.; Chaudhary, A.; Lumb, A.; Nand, B. *Green Chem.* **2012**, *14*, 2321.
- (14) Podlesny, E. E.; Carroll, P. J.; Kozlowski, M. C. *Org. Lett.* **2012**, *14*, 4862.
- (15) Bamfield, P.; Hutchings, M. G. *Chromic Phenomena. Technological Applications of Colour Chemistry*, 2nd ed.; The Royal Society of Chemistry: Cambridge, U.K., 2010.
- (16) See Supporting Information for details.
- (17) Somei, H.; Asano, Y.; Yoshida, T.; Takizawa, S.; Yamataka, H.; Sasai, H. *Tetrahedron Lett.* **2004**, *45*, 1841.

- (18) Guo, Q.-X.; Wu, Z.-J.; Luo, Z.-B.; Liu, Q.-Z.; Ye, J.-L.; Luo, S.-W.; Cun, L.-F.; Gong, L.-Z. *J. Am. Chem. Soc.* **2007**, *129*, 13927.
- (19) Takizawa, S.; Katayama, T.; Sasai, H. *Chem. Commun.* **2008**, 4113.
- (20) Takizawa, S.; Katayama, T.; Somei, H.; Asano, Y.; Yoshida, T.; Kameyama, C.; Rajesh, D.; Onitsuka, K.; Suzuki, T.; Mikami, M.; Yamataka, H.; Jayaprakash, D.; Sasai, H. *Tetrahedron* **2008**, *64*, 3361.
- (21) Takizawa, S.; Katayama, T.; Kameyama, C.; Onitsuka, K.; Suzuki, T.; Yanagida, T.; Kawai, T.; Sasai, H. *Chem. Commun.* **2008**, 1810.
- (22) Karikomi, M.; Yamada, M.; Ogawa, Y.; Houjou, H.; Seki, K.; Hiratani, K.; Haga, K.; Uyehara, T. *Tetrahedron Lett.* **2005**, *46*, 5867.
- (23) Nakano, K.; Hidehira, Y.; Takahashi, K.; Hiyama, T.; Nozaki, K. *Angew. Chem., Int. Ed.* **2005**, *44*, 7136.
- (24) Gingras, M.; Dubois, F. *Tetrahedron Lett.* **1999**, *40*, 1309.
- (25) Fox, J. M.; Katz, T. J. *J. Org. Chem.* **1999**, *64*, 302.
- (26) Hussain, H.; Specht, S.; Sarite, S. R.; Saefel, M.; Hoerauf, A.; Schulz, B.; Krohn, K. *J. Med. Chem.* **2011**, *54*, 4913.
- (27) Jiery, L.; Harthong, S.; Aronica, C.; Mulatier, J.-C.; Guy, L.; Guy, S. *Org. Lett.* **2012**, *14*, 288.
- (28) Gaiao, E. N.; Martins, V. L.; Lyra, W. S.; Almeida, L. F.; Sílvia, E. C.; Araújo, M. C. U. *Anal. Chim. Acta* **2006**, *570*, 283.
- (29) Martinez, A.; Phillips, S. T.; Carrilho, E.; Thomas, S. W., III; Sindi, H.; Whitesides, G. M. *Anal. Chem.* **2008**, *80*, 3699.
- (30) Baker, M. S.; Phillips, S. T. *Org. Biomol. Chem.* **2012**, *10*, 3595.
- (31) Mataka, S.; Moriyama, H.; Sawada, T.; Takahashi, K.; Sakashita, H.; Tashiro, M. *Chem. Lett.* **1996**, 363.
- (32) Long, S.; Parkin, S.; Siegler, M. A.; Cammers, A.; Li, T. *Cryst. Growth Des.* **2008**, *8*, 4006.
- (33) Sheth, A. R.; Lubach, J. W.; Munson, E. J.; Muller, F. X.; Grant, D. J. *J. Am. Chem. Soc.* **2005**, *127*, 6641.
- (34) Jenkins, R.; Snyder, R. L. *Introduction to X-ray Powder Diffractometry*; Wiley & Sons: New York, 1996; Chapter 12.
- (35) Banerjee, R.; Desiraju, G. R.; Mondal, R.; Howard, J. A. K. *Chem.—Eur. J.* **2004**, *10*, 3373.
- (36) Aullón, G.; Bellamy, D.; Brammer, L.; Bruton, E. A.; Orpen, A. G. *Chem. Commun.* **1998**, 653.
- (37) Taylor, M. S.; Jacoben, E. N. *Angew. Chem., Int. Ed.* **2006**, *45*, 1520.
- (38) Pucci, A.; Ruggeri, G. *J. Mater. Chem.* **2011**, 8282.
- (39) Davis, D. A.; Hamilton, A.; Yang, J.; Cremer, L. D.; Gough, D. V.; Potisek, S. L.; Ong, M. T.; Braun, P. V.; Martínez, T. J.; White, S. R.; Moore, J. S.; Sottos, N. R. *Nature* **2009**, *459*, 68.
- (40) Zhang, X.; Zhanguo, C.; Zhang, Y.; Liu, S.; Xu, J. *J. Mater. Chem. C* **2013**, *1*, 3376.
- (41) Kishimura, A.; Yamashita, T.; Yamaguchi, K.; Aida, T. *Nat. Mater.* **2005**, *4*, 546.
- (42) Ito, H.; Saito, T.; Oshima, N.; Kitamura, N.; Ishizaka, S.; Hinatsu, Y.; Wakeshima, M.; Kato, M.; Tsuge, K.; Sawamura, M. *J. Am. Chem. Soc.* **2008**, *130*, 10044.